

JOURNAL OF THE AMERICAN CHEMICAL SOCIETY

Electronic Characteristics of Arylated Tetraethynylethenes: A Cooperative Computational and Electrochemical Investigation

Anouk Hilger,[†] Jean-Paul Gisselbrecht,[‡] Rik R. Tykwinski,[§] Corinne Boudon,[‡] Martin Schreiber,[§] Rainer E. Martin,[§] Hans Peter Lüthi,^{*,†} Maurice Gross,^{*,‡} and François Diederich^{*,§}

Contribution from the Swiss Center for Scientific Computing, ETH-Zentrum, Clausiusstrasse 59, CH-8092 Zürich, Switzerland, Laboratoire d'Electrochimie et de Chimie Physique du Corps Solide, URA 405 au CNRS, Université Louis Pasteur, 4 rue Blaise Pascal, F-67000 Strasbourg, France, and Laboratory for Organic Chemistry, ETH-Zentrum, Universitätstrasse 16, CH-8092 Zürich, Switzerland

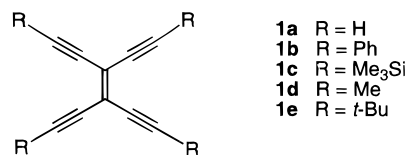
Received August 5, 1996[⊗]

Abstract: A systematic analysis of a series of donor- and/or acceptor-substituted tetraethynylethenes (TEEs, TEE = 3,4-diethynylhex-3-ene-1,5-diyne) was conducted by means of electrochemical analysis and *ab initio* calculations to determine the ability of the conjugated carbon core to promote electronic communication between pendant functionality. The electronic behavior as a function of the degree and pattern of substitution was examined and compared to the theoretical results. Experimentally, the study indicates that the electrochemically generated charges localize, since the presence of one redox center on the TEE core has a minimal effect on the redox characteristics of the other centers. Upon reduction of *p*-nitrophenyl-substituted TEEs, however, a decrease in bond length alternation in the TEE core and a corresponding increase in the phenyl rings were predicted by *ab initio* calculations. This cumulenic/quinoid structure was validated experimentally by the electrochemical isomerization of *cis*-1,6-bis(4-nitrophenyl)-3,4-bis{[(*tert*-butyldimethylsilyloxy)methyl]}hex-3-ene-1,5-diyne to its *trans*-isomer during cyclic voltammetry. Thus, the findings show that although the multiple *p*-nitrophenyl redox centers present on the TEE core apparently behave independently from one another in electrochemical reduction steps, delocalization of the incurred charges is effectively conveyed by the alkynes into the carbon framework. This delocalization imparts a sufficiently high single bond character to the central TEE double bond in the dianion to allow rotation and *cis*–*trans*-isomerization.

Introduction

Tetraethynylethene (TEE, 3,4-diethynylhex-3-ene-1,5-diyne, **1a**) and its derivatives (Chart 1) represent a class of two-dimensionally conjugated building blocks that provide a versatile “molecular construction kit” for the assembly of carbon-rich nanoarchitectures.^{1–5} These unique molecules combine amazing synthetic flexibility with a rigidly planar, unencumbered frame-

Chart 1



work that has readily been elaborated into acyclic⁶ and cyclic⁷

[†] Swiss Center for Scientific Computing, ETH-Zentrum.

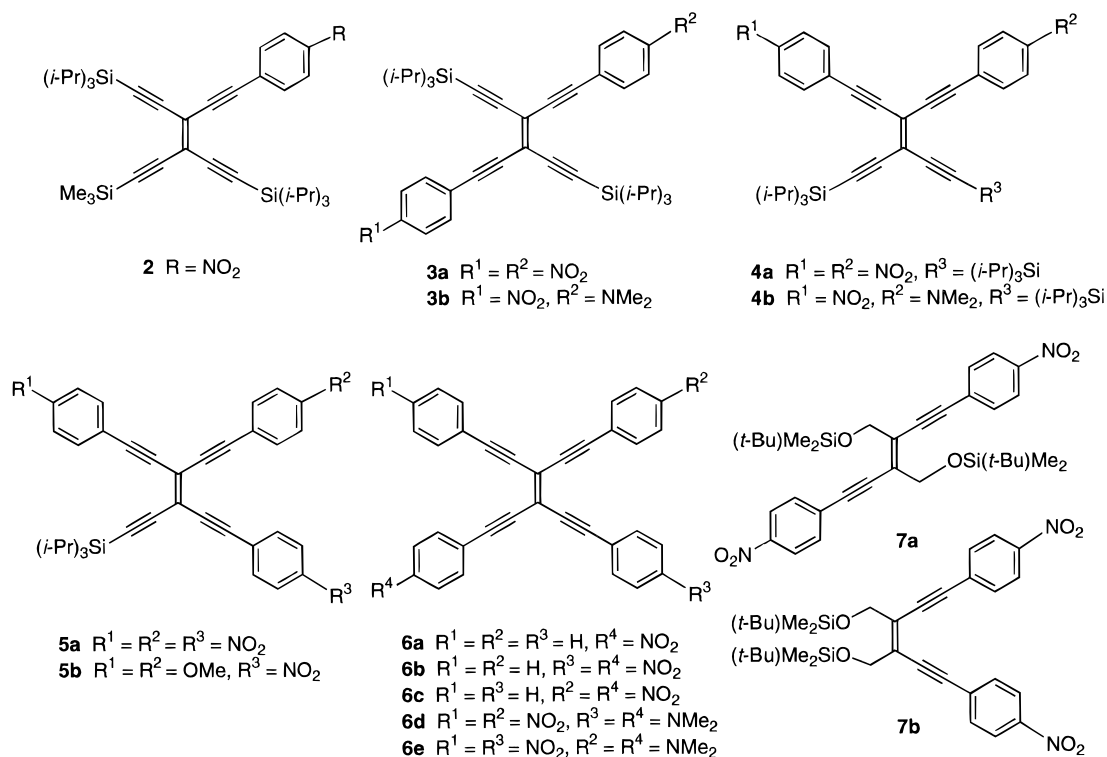
[‡] Université Louis Pasteur.

[§] Laboratory for Organic Chemistry, ETH-Zentrum.

[⊗] Abstract published in *Advance ACS Abstracts*, February 15, 1997.

(1) Diederich, F. *Nature (London)* **1994**, 369, 199–207. Diederich, F.; Rubin, Y. *Angew. Chem.* **1992**, 104, 1123–1146; *Angew. Chem., Int. Ed. Engl.* **1992**, 31, 1101–1123.

Chart 2



acetylenic molecular scaffolding, as well as oligomers and polymers with the conjugated poly(triacetylene) backbone.⁸

More recently, the interaction of perphenylated TEE, **1b**, with π -acceptors was shown to lead to highly ordered charge transfer complexes in the solid state and in solution.⁹ Electron rich (donor) and electron deficient (acceptor) groups have been attached to the planar TEE chromophore to broaden their applicability as materials for electronics and photonics. Thus, from a small number of selectively silyl protected precursors, a comprehensive library of donor/acceptor-substituted TEEs such as compounds **2–7** (Chart 2) has been assembled.^{10,11}

Structure–function investigations of TEEs have identified chromophore elements that correlate most closely with the

observed physical properties. For example, acentricity, donor/acceptor strength, and full two-dimensional conjugation were shown to significantly influence the third-order nonlinear optical properties.¹² Analysis of the second-order nonlinearity has identified similar structural motifs toward optimization of first-order hyperpolarizabilities.¹³ Throughout our studies, it has become clear that the observed physical properties propagate with the extension of the conjugated TEE enediyne chromophore. The successful evolution of organic materials based on TEEs requires a broad understanding of their ability to effectively function as a conjugated tether. In this study we have therefore examined the electrochemical behavior of a selected series of functionalized TEEs both experimentally and theoretically.

The electrochemistry of nitroaromatic molecules has been extensively studied.^{14–19} Pioneering work by Ammar and Savéant showed that, even in the presence of a conjugated bridge between two nitrophenyl groups, the difference between the first two reduction potentials rapidly decreases as the length of the bridge is increased.¹⁹ This study also showed that tetrakis(*p*-nitrophenyl)ethylene is reduced in two successive, reversible

(2) Hori, Y.; Noda, K.; Kobayashi, S.; Taniguchi, H. *Tetrahedron Lett.* **1969**, 3563–3566.

(3) Hauptmann, H. *Angew. Chem.* **1975**, *87*, 490–491; *Angew. Chem., Int. Ed. Engl.* **1975**, *14*, 498–499.

(4) Hopf, H.; Kreutzer, M.; Jones, P. G. *Chem. Ber.* **1991**, *124*, 1471–1475.

(5) (a) Rubin, Y.; Knobler, C. B.; Diederich, F. *Angew. Chem.* **1991**, *103*, 708–710; *Angew. Chem., Int. Ed. Engl.* **1991**, *30*, 698–700. (b) Anthony, J.; Boldi, A. M.; Rubin, Y.; Hobi, M.; Gramlich, V.; Knobler, C. B.; Seiler, P.; Diederich, F. *Helv. Chim. Acta* **1995**, *78*, 13–45. (c) Tykwinski, R. R.; Diederich, F.; Gramlich, V.; Seiler, P. *Helv. Chim. Acta* **1996**, *79*, 634–645.

(6) Boldi, A. M.; Anthony, J.; Gramlich, V.; Knobler, C. B.; Boudon, C.; Gisselbrecht, J.-P.; Gross, M.; Diederich, F. *Helv. Chim. Acta* **1995**, *78*, 779–796.

(7) Anthony, J.; Boldi, A. M.; Boudon, C.; Gisselbrecht, J.-P.; Gross, M.; Seiler, P.; Knobler, C. B.; Diederich, F. *Helv. Chim. Acta* **1995**, *78*, 797–817.

(8) Schreiber, M.; Anthony, J.; Diederich, F.; Spahr, M. E.; Nesper, R.; Hubrich, M.; Bommeli, F.; Degiorgi, L.; Wachter, P.; Kaatz, P.; Bosshard, C.; Günter, P.; Colussi, M.; Suter, U. W.; Boudon, C.; Gisselbrecht, J.-P.; Gross, M. *Adv. Mater.* **1994**, *6*, 786–790.

(9) (a) Diederich, F.; Philp, D.; Seiler, P. *J. Chem. Soc., Chem. Commun.* **1994**, 205–208. (b) Philp, D.; Gramlich, V.; Seiler, P.; Diederich, F. *J. Chem. Soc., Perkin Trans. 2* **1995**, 875–886. (c) Taniguchi, H.; Hayashi, K.; Nishioka, K.; Hori, Y.; Shiro, M.; Kitamura, T. *Chem. Lett.* **1994**, 1921–1924.

(10) Tykwinski, R. R.; Schreiber, M.; Gramlich, V.; Seiler, P.; Diederich, F. *Adv. Mater.* **1996**, *8*, 226–231.

(11) Tykwinski, R. R.; Schreiber, M.; Perez-Carlón, R.; Diederich, F.; Gramlich, V.; Seiler, P. *Helv. Chim. Acta* **1996**, *79*, 2249–2281.

(12) Bosshard, Ch.; Spreiter, R.; Günter, P.; Tykwinski, R. R.; Schreiber, M.; Diederich, F. *Adv. Mater.* **1996**, *8*, 231–234.

(13) Spreiter, R.; Bosshard, Ch.; Knöpfle, G.; Günter, P.; Tykwinski, R. R.; Schreiber, M.; Diederich, F. *J. Phys. Chem.*, submitted for publication.

(14) Kemula, W.; Krygowski, T. M. In *Encyclopedia of Electrochemistry of the Elements*; Bard, A. J., Lund, H. Eds.; M. Dekker: New York, 1979; Organic Section, Vol. XIII, Chapter 2. Maki, A. H.; Geske, D. H. *J. Am. Chem. Soc.* **1961**, *83*, 1852–1860. Geske, D. H.; Maki, A. H. *J. Am. Chem. Soc.* **1960**, *82*, 2671–2676.

(15) Jensen, B. S.; Parker, V. D. *J. Chem. Soc., Chem. Commun.* **1974**, 367–368.

(16) Krygowski, T. M.; Stencel, M.; Galus, Z. *J. Electroanal. Chem.* **1972**, *39*, 395–405.

(17) Geske, D. H.; Ragle, J. L.; Bambenek, M. A.; Balch, A. L. *J. Am. Chem. Soc.* **1964**, *86*, 987–1002.

(18) Kitagawa, T.; Ichimura, A. *Bull. Chem. Soc. Jpn.* **1973**, *46*, 3792–3795. Lawless, J. G.; Bartak, D. E.; Hawley, M. D. *J. Am. Chem. Soc.* **1969**, *91*, 7121–7127. Peover, M. E. *Trans. Faraday Soc.* **1964**, *60*, 479–483.

(19) Ammar, F.; Savéant, J. M. *J. Electroanal. Chem.* **1973**, *47*, 115–125.

two-electron reductions; first, a two-electron transfer to *gem*-oriented *p*-nitrophenyl moieties, and then a two-electron reduction of the remaining two nitrophenyl groups. The redox behavior of alkyne-linked 2,5-bis(*N,N*-diethylamino)phenyl groups reported by Zhou and Swager²⁰ has shown that electrochemically generated radical cations and dications are highly localized. These observations suggested an inability of the conjugated framework to participate in charge delocalization. The electrochemical reduction of stilbenes, however, confirmed partial charge delocalization by demonstrating *cis*–*trans*-isomerization as a result of reduced olefinic bond order.²¹ Additionally, electrochemical analyses of tetraphenylethenes also showed charge delocalization, resulting in both diminished bond order of the olefin and marked structural rearrangements to relieve steric and electrostatic interactions.²²

Our electrochemical analyses of donor- and/or acceptor-functionalized TEEs initially appeared to echo reports for similar conjugated systems which predicted highly localized redox centers. A rigorous *ab initio* examination,²³ however, revealed a much more complex picture. We now report the conclusions of this combined investigation which detail the influences of linear and cross-conjugation and clearly outline the ability of the conjugated TEE enediyne core to effectively promote conjugation.

Results and Discussion

Electrochemistry. (a) Redox Behavior of *p*-Nitrophenyl Derivatives. All species examined in the present study were electroactive within the available potential range in CH₂Cl₂ + 0.1 M Bu₄NPF₆ and gave well-defined signals with the exception of **6a**, **6b**, and **6e** (Table 1). The latter three molecules gave no well-defined reduction on a rotating disk electrode (RDE) due to adsorption and electrode inhibition phenomena; however, on the time scale of cyclic voltammetry (CV), these species could be analyzed and gave well-resolved cyclovoltammograms (CVs). Of all the mono- and bis(nitrophenyl) derivatives examined, none were oxidized over the available potential range with the exception of **6a**, which was oxidized at +1.15 V *vs* ferrocene (V/Fc). All species gave several reduction steps, as demonstrated by the CVs shown in Figure 1 for a selected series of mono- (**6a**), bis- (**6b** and **6c**), and tris(nitrophenyl) (**5a**) derivatives. The first reduction step characteristically occurred at an average potential of –1.37 V/Fc.

Steady state voltammetry (SSV) gave well-defined voltammograms for all species with the exception of **6a**, **6b**, and **6e**, where electrode inhibition hindered a detailed study. For all mono- and bis(nitrophenyl)-substituted TEEs, including those with additional anisyl or aniline functionality, the first reduction wave had an amplitude proportional to the number of nitrophenyl groups present in the molecule. Wave analysis for **2**, **3a**, and **6c** gave slopes close to 70 mV (uncorrected for ohmic drop), values indicative of reversible one-electron reductions. For **3a** and **6c**, however, the wave amplitudes were twice those of **2** and **6a**, and wave analyses were in agreement with the presence of two overlapping and independent reduction events,

Table 1. Electrochemical Data for Functionalized Tetraethynylethenes **1–6** and the Enediynes **7a/b**^a

compd	cyclic voltammetry			rotating disk electrode				
	<i>E</i> ^o <i>vs</i> Fc ^b (V)	Δ <i>E</i> _p ^c (mV)	<i>E</i> _{pc} <i>vs</i> Fc ^d (V)	<i>E</i> _{1/2} <i>vs</i> Fc (V)	slope ^e (mV)	no. of electrons		
1b ^f	–1.76	155 ^g		–1.77	60	1		
				–2.11	70			
				–2.32	80			
1e ^f	–1.96	320 ^g		–2.02	60	1		
				–2.50	80			
				–2.74	160			
2	–1.36	75		–1.37	68	1		
				–1.65	75	68	1	
3a	–1.35	85		–1.37	67	2		
				–1.73	85	–1.77	62	1
3b	–1.40	85	–2.28	–1.42	75	1		
				–1.73	70	–1.76	66	1
				+0.47	75	+0.47	68	1
4a	–1.38	100		–1.38	92	2		
				–1.65	73	–1.71	63	1
4b	–1.37	80	–2.08	–1.39	66	1		
				–1.68	70	–1.71	63	1
				+0.46	65	+0.46	59	1
5a	–1.26	84	<i>h</i>	–1.29	59	2		
				–1.43	84	–1.49	53	1
				–1.71	100			1
5b	–1.38	80		–1.39	76	1		
				–1.69	69	–1.69	69	1
				–1.65	80	+0.96	71	2
6a	–1.34	90		<i>i</i>		1		
				–1.53	85			1
6b	–1.38	150		+1.19	91			
				–1.57	120	<i>ca.</i> –1.38	<i>j</i>	2
6c	–1.29	84		<i>ca.</i> –1.57	<i>j</i>	1		
				–1.64	100	–2.17		
6d	–1.38	80		–1.33	61	2		
				–1.69	105	–1.71	58	1
						–2.20		
6e	–1.38	95		–2.11	113	1		
				–1.76	110	+0.46	60 ^k	2
						–1.32	66	2
7a	–1.42	120		<i>l</i>		1		
						–2.22		
						+0.40	+0.41	122
7b	–1.40	100		–1.45	100	2		
				–2.16	180	–2.12	180	1
				–2.09	115	–1.44	100	2
			–2.09	115	1			

^a Redox potentials observed in CH₂Cl₂ + 0.1 M Bu₄NPF₆ on glassy carbon. ^b Formal redox potential $E^{\circ} = (E_{pa} + E_{pc})/2$. ^c At scan rate 100 mV s^{–1}. ^d Peak potentials for irreversible reductions and oxidations. ^e Logarithmic analysis of the wave obtained by plotting E *vs* log[$I/I_{lim} - I$]. ^f Reduction potentials observed in THF + 0.1 M Bu₄NPF₆ at a Hg working electrode (ref 27). ^g At scan rate 10 V s^{–1}. ^h Reversible at scan rate > 2 V s^{–1}. ⁱ Not well-defined. ^j Poorly resolved wave. ^k Adsorption. ^l Polarographic maximum.

namely, the reduction of the two nitrophenyl groups. This conclusion was confirmed by CV for **3a** and **6c**, where the observed reductions were reversible ($I_{pa}/I_{pc} = 1$ at all sweep rates) and the peak potential differences measured at 0.1 V s^{–1} were close to 80 mV (uncorrected for ohmic drop), values in agreement with the reductions of two independent redox centers.

Optically transparent thin layer electrode (OTTLE) studies of the first reduction steps for **3a**, **6a**, and **6c** gave nice spectral evolutions with well-defined isosbestic points. For the mono-(nitrophenyl) derivative **6a**, Figure 2a shows an absorption at 668 nm for the reduced species, characteristic of a reduced

(20) Zhou, Q.; Swager, T. M. *J. Org. Chem.* **1995**, *60*, 7096–7100.

(21) Chien, C. K.; Wang, H. C.; Szwarc, M.; Bard, A. J.; Itaya, K. *J. Am. Chem. Soc.* **1980**, *102*, 3100–3104. Wang, H. C.; Levin, G.; Szwarc, M. *J. Am. Chem. Soc.* **1977**, *99*, 2642–2647. Sorensen, S.; Levin, G.; Szwarc, M. *J. Am. Chem. Soc.* **1975**, *97*, 2341–2345. Ward, T. A.; Levin, G.; Szwarc, M. *J. Am. Chem. Soc.* **1975**, *97*, 258–261.

(22) Wolf, M. O.; Fox, H. H.; Fox, M. A. *J. Org. Chem.* **1996**, *61*, 287–294. Shultz, D. A.; Fox, M. A. *J. Org. Chem.* **1990**, *55*, 1047–1051. Fox, M. A.; Shultz, D. A. *J. Org. Chem.* **1988**, *53*, 4386–4390.

(23) For previous *ab initio* studies of **1a** see: Ma, B.; Xie, Y.; Schaefer, H. F. *Chem. Phys. Lett.* **1992**, *191*, 521–526. Ma, B.; Sulzbach, H. M.; Xie, Y.; Schaefer, H. F. *J. Am. Chem. Soc.* **1994**, *116*, 3529–3538.

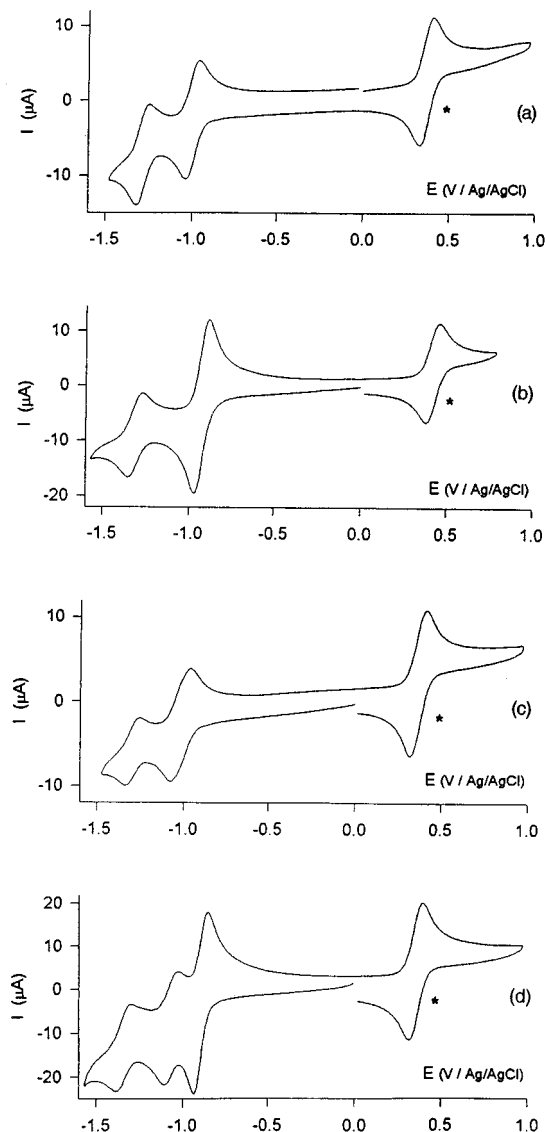


Figure 1. Cyclic voltammetry on a glassy carbon electrode in $\text{CH}_2\text{Cl}_2 + 0.1 \text{ M Bu}_4\text{NPF}_6$ at 0.1 V s^{-1} for (a) **6a**, (b) **6b**, (c) **6c**, and (d) **5a** (the asterisk refers to the Fc/Fc^+ couple used as an internal standard).

nitrophenyl moiety.²⁴ For **6c** containing two nitrophenyl groups, Figure 2b shows that the reduced species gave rise to bands at 560 and 606 nm, as well as a low-energy absorption above 820 nm. The presence of clear isosbestic points in Figure 2b indicated that both nitrophenyl groups were reduced and no intermediate species could be observed on the time scale of the OTTLE measurements; *i.e.*, the two nitrophenyl groups in **6c** behaved as two independent redox centers. In each case, reversibility was confirmed as the initial absorption spectrum could be quantitatively recovered through reoxidation.

The *gem*-bis(nitrophenyl) TEEs **4a** and **6b** both gave satisfactory CV results; however, only **4a** gave a well-defined wave in SSV. Even at slow sweep rates, the peak potential differences for **4a** and **6b** (100 and 150 mV, respectively) were somewhat higher than 60 mV, expected for a reversible one-electron charge transfer. It was, however, possible to estimate the redox potential difference existing between the two consecutive and overlapping charge transfers from the peak shape. Thus, from the $E_p - E_{p/2}$ values of 90 and 100 mV, calculated values of 70

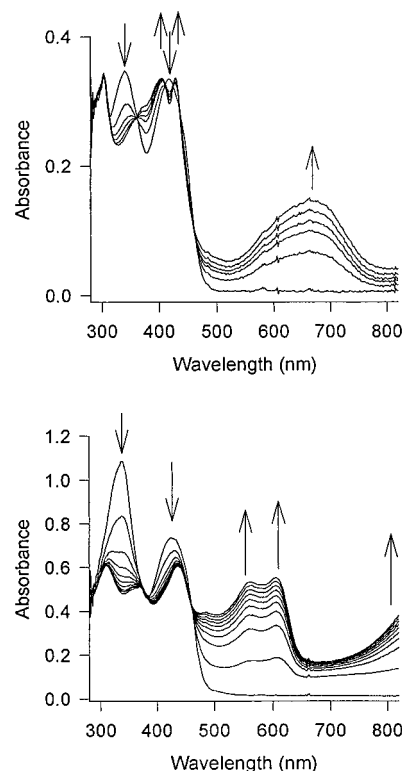


Figure 2. Time-resolved UV/vis spectra for OTTLE reduction in $\text{CH}_2\text{Cl}_2 + 0.1 \text{ M Bu}_4\text{NPF}_6$ of (a, top) **6a** and (b, bottom) **6c**.

and 75 mV were obtained²⁵ as the difference between the first two reductions of **4a** and **6b**, respectively. These values were in good agreement with the calculated redox potential obtained by SSV from the slope of the first reduction wave. OTTLE experiments on **4a** clearly showed that it was possible to electrogenerate either the radical anion or dianion due to the potential difference existing between the two overlapping charge transfers (Figure 3). The reduction of one nitrophenyl group gave a single band at 604 nm, whereas the dianion displayed two bands at 572 and 612 nm, analogous to the results for **6c** shown in Figure 2b.

Finally, the presence of (*N,N*-dimethylamino)phenyl or anisyl donor substituents on the TEE core had little effect on the first reduction potential involving the nitrophenyl groups as clearly demonstrated by examination of the redox behavior of donor/acceptor systems **3b**, **4b**, **5b**, **6d**, and **6e** which all gave first reduction potentials of *ca.* $-1.38 \text{ V}/\text{Fc}$.²⁶

All mono- and bis(nitrophenyl)-substituted TEEs displayed a second reduction step at *ca.* $-1.6 \text{ V}/\text{Fc}$, corresponding to a charge transfer to the tetraethynylethene carbon framework. This reduction step to the TEE core is corroborated by comparison to the redox behavior of tetrakis(phenylethynyl)ethene, **1b**,²⁷ where the absence of donor/acceptor functionality results in a reversible one-electron transfer at $-1.68 \text{ V}/\text{Fc}$, very close to the second potentials observed for the nitrophenyl species.

Analysis of the second reduction potentials observed for the one-electron transfer to the TEE core of nitrophenyl derivatives revealed that the values for this redox step are dependent upon both orientation of the substituents about the TEE core and the nature of the other substituents present (*i.e.*, (*i*-Pr)₃Si *vs* Ph).

(25) Myers, R. L.; Shain, I. *Anal. Chem.* **1969**, *41*, 980.

(26) See the Supporting Information for a complete description of the redox properties of *p*-(*N,N*-dimethylamino)phenyl- and *p*-anisyl-substituted TEEs.

(27) Boudon, C.; Gisselbrecht, J.-P.; Gross, M.; Anthony, J.; Boldi, A. M.; Faust, R.; Lange, T.; Philip, D.; Van Loon, J.-D.; Diederich, F. *J. Electroanal. Chem.* **1995**, *394*, 187–197.

(24) Constantinescu, E.; Hillebrand, M.; Volanschi, E.; Wendt, H. *J. Electroanal. Chem.* **1988**, *256*, 95–109. Osa, T.; Kuwana, T. *J. Electroanal. Chem.* **1969**, *22*, 389–406. Kemula, W.; Sioda, R. *J. Electroanal. Chem.* **1964**, *7*, 233–241.

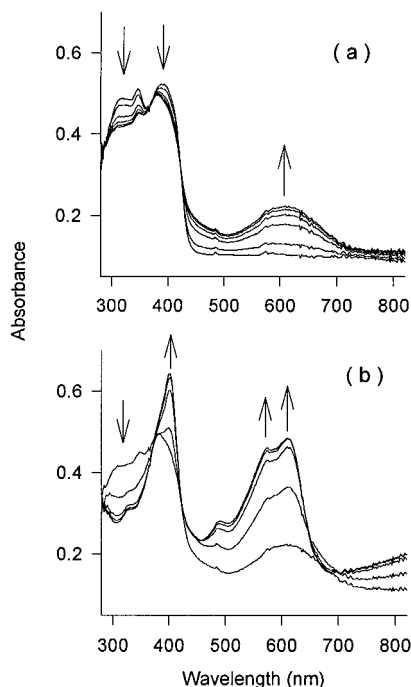


Figure 3. Time-resolved UV/vis spectra for the OTTLE reduction of **4a** in $\text{CH}_2\text{Cl}_2 + 0.1 \text{ M Bu}_4\text{NPF}_6$ at (a) -1.35 V/Fc (just below half wave potential) and (b) -1.45 V/Fc (plateau potential).

For example, comparison of the perarylated series **6a**, **6b**, and **6c** to the analogous silyl-substituted series **2**, **4a**, and **3a** demonstrates that reductions in the latter are 120, 80, and 90 mV, respectively, more difficult than in the former series. This is in good agreement with the expectation that extension of the conjugated π -electron framework upon introduction of phenyl groups should lower the energy of the lowest unoccupied molecular orbital (LUMO).

Pairwise comparison of (**2**, **6a**), (**4a**, **6b**), and (**3a**, **6c**) clearly demonstrates the effects of substitution pattern on the redox behavior and substantiates the ability of the acetylenic moieties to participate in delocalization of the incurred charge. The second reduction occurs at -1.65 V/Fc for (**2**, **4a**), and at -1.55 V/Fc for (**6a**, **6b**), whereas it is observed at -1.73 and -1.64 V/Fc for **3a** and **6c**, respectively. The occurrence of the second reduction at similar potentials for analogous pairs of radical anions (**2**, **6a**) and dianions (**4a**, **6b**) suggests that the geminal orientation of the nitrophenyl groups in the latter somewhat limits the possibility of delocalization into the carbon core due to the cross-conjugated orientation of the anionic centers. Furthermore, comparison of *gem*-derivatives (**4a**, **6b**) to the *trans*-derivatives (**3a**, **6c**) shows the reduction of the latter to be *ca.* 80 mV more difficult. Orientation of the nitrophenyl groups of **3a** and **6c** in a linear manner facilitates charge delocalization into the core, and thus augments the energetic requirements for the second reduction step.

(b) Redox Behavior of Tris(nitrophenyl) Derivative 5a. The redox behavior of this molecule differs considerably from that of the nitrophenyl series discussed above and requires individual attention. The first reversible reduction at -1.26 V/Fc involved two electrons, whereas the second and third reductions at -1.43 and -1.71 V/Fc , respectively, were each reversible, one-electron transfer events (Table 1). The first reduction corresponds to electron transfers involving two independent redox centers as observed previously for bis-(nitrophenyl) derivatives, albeit at a potential 100 mV more positive. The second reduction, also occurring at a nitrophenyl group, is *ca.* 50 mV more negative than the average *first*

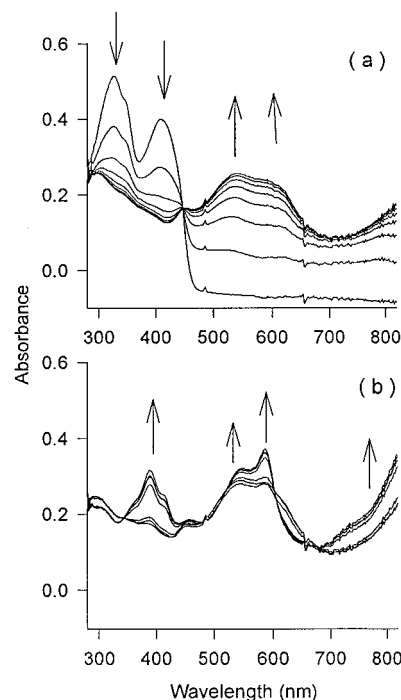


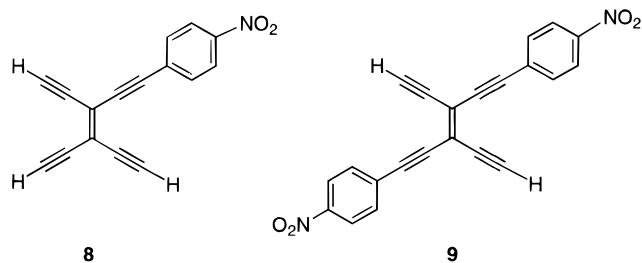
Figure 4. Time-resolved UV/vis spectra for the OTTLE reduction of **5a** in $\text{CH}_2\text{Cl}_2 + 0.1 \text{ M Bu}_4\text{NPF}_6$ at (a) -1.35 V/Fc (first reduction plateau potential) and (b) -1.45 V/Fc (second reduction plateau potential).

reduction potential of the mono- and bis(nitrophenyl) TEEs. OTTLE experiments confirmed that the first and second reductions involved the nitrophenyl groups as the absorption bands at 540 and 588 nm observed after the first reduction (Figure 4a) were only slightly shifted to 548 and 588 nm after the second reduction (Figure 4b). The third reduction step, the transfer of an electron to the TEE carbon core, is more difficult, occurring at -1.71 V/Fc , as would be expected for electron transfer to such a highly charged species.

Computational Studies. (a) Computational Details. The computations presented in this work focus on the investigation of the molecular and electronic structure (ground state) of neutral mono(nitrophenyl)-3,4-diethynylhex-3-ene-1,5-diyne, **8**, and its radical anion, *trans*-1,6-bis(*p*-nitrophenyl)-3,4-diethynylhex-3-ene-1,5-diyne, **9**, as well as its radical anion and dianion (Chart 3).

The geometries of **8** and **9** were optimized using the 6-31G** basis set. Single-point energy calculations of **9** were then performed at the geometry obtained at the HF/6-31G** level using extended basis sets (i.e., HF/PVDZa/HF/6-31G**). From validation studies (Hartree–Fock theory) on the molecular structures and electron affinities of TEE and nitrobenzene (Supporting Information), it appeared that a polarization function along with a diffuse p-type function is necessary when investigating the *electronic* structure of the anions of **8** and **9**. Additional diffuse s- and d-functions, however, did not seem to be critical components and were therefore omitted. For the *molecular* structure computations, the basis set requirements are less strict and the HF/6-31G** level of theory is appropriate. For the computations of the electron affinities of **9**, a modified 6-31+G* basis set and the (9s4p1d/4s1p)[3s2p1d/2s1p] polarized valence double- ζ correlation consistent basis sets of Dunning,²⁸ denoted PVDZ and PVDZa, were employed. The modified 6-31+G* and PVDZa basis sets are both augmented with a diffuse p-exponent (but no diffuse s- and

Chart 3



d-functions) on the heavy atoms. The modified 6-31+G* and PVDZa (9s5p1d/4s1p)[3s3p1d/2s1p] working basis sets for **9** consisted of a total of 496 and 554 contracted basis functions, respectively.

All calculations were carried out using the restricted Hartree–Fock (RHF) and restricted open-shell Hartree–Fock (ROHF) schemes. Furthermore, density functional theory (DFT) with a B3LYP²⁹ functional was used to investigate the electron affinities of **9**.

Unless otherwise noted, D_{2h} symmetry was applied for TEE, C_s symmetry for **8**, and C_{2h} symmetry for **9**. The programs used were the Gaussian 94 package,³⁰ DISCO,³¹ and TURBO-MOLE.³²

(b) Molecular Structures. The optimized molecular geometries play a vital role in the interpretation of electronic properties. The computed equilibrium geometries at the HF/6-31G** level of theory of the neutral compounds **8** and **9** and their anions are presented in Tables 2 and 3.

First, considering the computed structure of the carbon scaffold for the neutral species, the bond lengths found for the mono(nitrophenyl) compound **8** and the bis(nitrophenyl) derivative **9** lie in the same range as those predicted for the parent TEE (Supporting Information), which means that all bond lengths are close to the standard values for single, double, and triple bonds (1.433 Å vs 1.43 Å for $C_{sp^2}-C_{sp}$, 1.348 Å vs 1.34 Å for $C=C$, and 1.190 Å vs 1.182 Å for $C\equiv C$).³³ Thus, the enediyne character is dominant in the neutral compounds, and as expected, little structural change upon substitution is observed for these molecules in the ground state.^{10,34,35}

An examination of the bond length alternations between the neutral and radical anion for monosubstituted **8** (Table 2) shows that the reduction process imparts little change on the core geometry. Whereas the central bonds *h* (figure in Table 3) of the parent TEE **1a**^{•-} and disubstituted **9**^{•-} (Tables 3 and 4) lengthen by 0.084 and 0.073 Å, respectively, a change of merely 0.009 Å is observed for **8**^{•-}.

Upon reduction to **9**²⁻, the bond length changes observed in **9** (Table 3) reveal a strong tendency of the core geometry toward

Table 2. HF/6-31G** Bond Lengths and Bond Length Differences (Å) of **8** and Radical Anion **8**^{•-}

bond ^a	l_{ne}^b	l_{ma}^c	Δl_{ma-ne}
<i>a</i>	1.458	1.368	-0.090
<i>b</i>	1.383	1.414	0.031
<i>c</i>	1.380	1.366	-0.014
<i>d</i>	1.394	1.409	0.015
N–O	1.194	1.249	0.055
<i>e</i>	1.437	1.415	-0.022
<i>f</i>	1.190	1.201	0.011
<i>g</i>	1.434	1.415	-0.019
<i>h</i>	1.347	1.356	0.009
<i>p</i>	1.438	1.443	0.005
<i>q</i>	1.187	1.187	0.000
<i>r</i>	1.057	1.056	-0.001
<i>e'</i>	1.057	1.056	-0.001
<i>f'</i>	1.187	1.189	0.002
<i>g'</i>	1.437	1.437	0.000
<i>p'</i>	1.438	1.436	-0.002
<i>q'</i>	1.187	1.189	0.002
<i>r'</i>	1.057	1.056	-0.001

^a Bond labels according to figure above. ^b ne designates the neutral species. ^c ma designates the monoanion.

Table 3. HF/6-31G** Bond Lengths and Bond Length Differences (Å) of **9**, Radical Anion **9**^{•-}, and Dianion **9**²⁻

bond ^a	l_{ne}^b	l_{ma}^c	l_{da}^d	Δl_{ma-ne}	Δl_{da-ma}	Δl_{da-ne}
<i>a, a'</i>	1.459	1.440	1.383	-0.019	-0.057	-0.076
<i>b, b'</i>	1.383	1.389	1.416	0.006	0.027	0.033
<i>c, c'</i>	1.380	1.374	1.353	-0.006	-0.021	-0.027
<i>d, d'</i>	1.394	1.406	1.443	0.012	0.037	0.049
N–O	1.193	1.200	1.220	0.007	0.020	0.027
<i>e, e'</i>	1.437	1.411	1.355	-0.026	-0.056	-0.082
<i>f, f'</i>	1.190	1.205	1.238	0.015	0.033	0.048
<i>g, g'</i>	1.433	1.399	1.345	-0.034	-0.054	-0.088
<i>h</i>	1.348	1.421	1.478	0.073	0.057	0.130
<i>p, p'</i>	1.438	1.429	1.435	-0.009	0.006	-0.003
<i>q, q'</i>	1.187	1.193	1.194	0.006	0.001	0.007
<i>r, r'</i>	1.057	1.055	1.055	-0.002	0.000	-0.002

^a Bond labels according to figure above. ^b ne designates the neutral species. ^c ma designates the monoanion. ^d da designates the dianion.

cumulenonic. The triple bonds *f* and *f'* along the conjugation path elongate by 0.048 Å, whereas the single bonds *g* and *g'* contract by 0.088 Å, so that both types of bonds show significant double bond character. The central double bond *h* (figure in Table 3) lengthens by as much as 0.130 Å in the dianion **9**²⁻, which indicates that this bond acquires strong single bond character. The bond length alternations of **9**²⁻ involve the entire substituted enediyne skeleton, whereas in the unsubstituted TEE **1a** (Table 4), only the central double bond is affected. This demonstrates that the presence of the two electron deficient nitrophenyl groups leads to a strong preference for a cumulenonic resonance structure in the reduced chromophores of **9**. It is interesting to note that the lengths of the bonds *p*, *p'*, *q*, *q'*, *r*, and *r'*, which are outside

(29) Becke, A. D. *J. Chem. Phys.* **1993**, *98*, 1372–1377.

(30) Gaussian 94, Revision C.3: Frisch, M. J.; Trucks, G. W.; Schlegel, H. B.; Gill, P. M. W.; Johnson, B. G.; Robb, M. A.; Cheeseman, J. R.; Keith, T. A.; Petersson, G. A.; Montgomery, J. A.; Raghavachari, K.; Al-Laham, M. A.; Zakrzewski, V. G.; Ortiz, J. V.; Foresman, J. B.; Cioslowski, J.; Stefanov, B. B.; Nanayakkara, A.; Challacombe, M.; Peng, C. Y.; Ayala, P. Y.; Chen, W.; Wong, M. W.; Andres, J. L.; Replogle, E. S.; Gomperts, R.; Martin, R. L.; Fox, D. J.; Binkley, J. S.; Defrees, D. J.; Baker, J.; Stewart, J. J. P.; Head-Gordon, M.; Gonzalez, C.; Pople, J. A., Gaussian, Inc., Pittsburgh, PA, 1995.

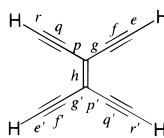
(31) DISCO, A Direct SCF and MP2 Code written by Almlöf, J.; Faegri, K.; Feyereisen, M. W.; Fischer, T. H.; Lüthi, H. P., ETH Zürich Version 3.0, 1994.

(32) Ahlrichs, R.; Bär, M.; Häser, M.; Horn, H.; Kölmel, Ch. *Chem. Phys. Lett.* **1989**, *162*, 165–169.

(33) Carey, F. A.; Sundberg, R. J. *Advanced Organic Chemistry*; Plenum Press: New York, 1984; Chapter 1.

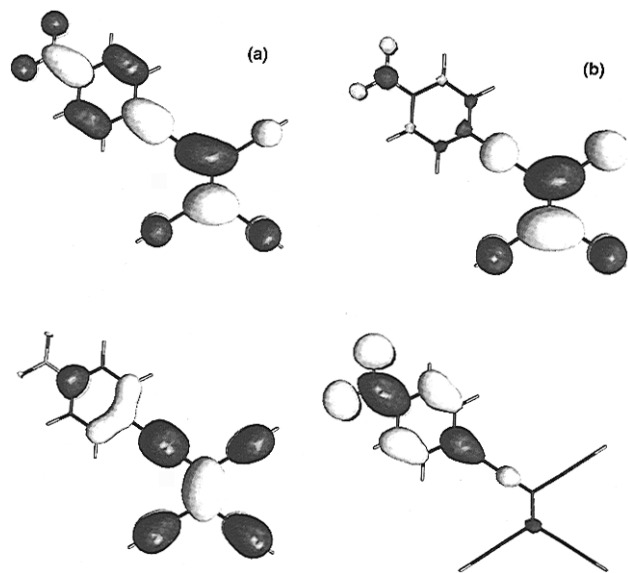
(34) Dehu, C.; Meyers, F.; Brédas, J. L. *J. Am. Chem. Soc.* **1993**, *115*, 6198–6206.

(35) Brédas, J. L.; Meyers, F. *Nonlinear Opt.* **1991**, *1*, 119–123.

Table 4. HF/6-31G** Bond Lengths and Bond Length Differences (Å) of **1a**, Radical Anion **1a^{•-}**, and Dianion **1a²⁻**


bond ^a	<i>l</i> _{ne} ^b	<i>l</i> _{ma} ^c	<i>l</i> _{da} ^d	Δl_{ma-ne}	Δl_{da-ma}	Δl_{da-ne}
<i>e, e', r, r'</i>	1.057	1.054	1.053	-0.003	-0.001	-0.004
<i>f, f', q, q'</i>	1.187	1.197	1.214	0.010	0.017	0.027
<i>g, g', p, p'</i>	1.438	1.421	1.399	-0.017	-0.022	-0.039
<i>h</i>	1.345	1.429	1.527	0.084	0.098	0.182

^a Bond labels according to figure above. ^b ne designates the neutral species. ^c ma designates the monoanion. ^d da designates the dianion.

**Figure 5.** Highest occupied molecular orbitals (HOMOs; bottom) and lowest unoccupied molecular orbitals (LUMOs; top) of (a) neutral **8** and (b) radical anion **8^{•-}**.

the main conjugation path, are affected neither by the substituents nor by the reduction process.

As the monosubstituted species **8** is reduced to **8^{•-}**, bond *a* (figure in Table 2) between the phenyl ring and the nitrogen atom contracts considerably ($\Delta l_{da-ne} = -0.090$ Å). Within the phenyl rings of **8**, the calculated bond lengths of the neutral molecule have benzoid character, whereas in the radical anion a quinoid-like structure is formed. Similar considerations apply for the dianion **9²⁻**. Analysis of the three computed structures (**9**, **9^{•-}**, **9²⁻**) shows that, when proceeding from the neutral to the dianion, the bond length alternation in the phenyl rings steadily increases so that the quinoid form dominates in the dianion. As an indicator for the extent of quinoid character in the phenyl rings, the degree of bond length alternation can be defined by the parameter in eq 1 (bond labels from the figure in Table 3).³⁴

$$\delta r = \frac{(b - c) + (d - c)}{2} = \frac{(b' - c') + (d' - c')}{2} \quad (1)$$

In benzene, the δr value equals 0, whereas values between 0.08 and 0.10 are found in a fully quinoid ring. In the analyses of **8** and **8^{•-}**, δr is 0.01 for the neutral species and 0.05 for the monoanion, whereas for **9** and its anions, δr is 0.01, 0.02, and 0.08, respectively, thus confirming the quinoid contribution to the anionic structures.

It can be concluded that, upon reduction of **8**, only the nitrophenyl substituent is affected and adopts a quinoid-like

form, whereas the TEE core remains unchanged. The reduction of **9** to **9²⁻**, however, involves both the nitrophenyl groups and the TEE frame, leading to cumulenyl/quinoid structures.

(c) **Electronic Structure and Energetics.** The changes in the molecular structures upon reduction can be qualitatively understood by inspection of the electronic structures of the different reduced states of **8** and **9**. For simplification, the present discussion is based on the shape of the molecular orbitals (MOs) (Figures 5 and 6) and the Mulliken charges (Table 5) for each compound at its respective equilibrium geometry.

Figure 5 shows that in **8^{•-}** the additional charge localizes on the nitrophenyl ring as one would expect from chemical intuition. For the disubstituted **9**, however, the first electron addition is strongly localized on the central ethylenic bond (bond *h* in Table 3) and, somewhat surprisingly, very little charge is found on the nitrophenyl groups (Figure 6b). Indeed, the HOMO of the radical anion **9^{•-}** shows strong π^* antibonding character for bond *h*, resulting in a lengthening of this bond. For the dianion **9²⁻** considerable charge is now also found on the nitrophenyl groups (Figure 6c), and the charge is more evenly distributed throughout the molecule.

It appears that the nitrophenyl groups in **9** enhance the local electron affinity of the central ethylenic bond, such that in the first reduction step the charge does not migrate onto the nitrophenyl units, but is accommodated mainly by bond *h*. Only in the second reduction step does accumulation of charge on the nitrophenyl groups become significant (Table 5).

The different behavior of compounds **8** and **9** with regard to reduction can be illustrated in terms of the forms and the ordering of the molecular orbitals: the LUMOs of both molecules in their neutral states show strong delocalization (Figures 5 and 6). Once reduced (*i.e.*, the LUMO is half-occupied and turns into the HOMO of the monoanion), a distinctly different situation is encountered. Both orbitals undergo localization, however, in opposite directions. The HOMO of **8^{•-}** localizes on the nitrophenyl unit, whereas the HOMO of **9^{•-}** localizes on the central ethylenic bond. Accordingly, the LUMOs of the monoanions show the complementary behavior. The strong electronic relaxation effects and the different relaxation paths involved make a prediction of properties based on inspection of the electronic structure of the neutral species very difficult.

In terms of polymer physics, the dianion structure, **9²⁻**, would be referred to as a bipolaron.³⁶ The alternative structure, namely, two independent polarons, would not be consistent with the cumulenyl TEE core and the low barrier to rotation about the central olefinic bond, observed in this study. In a two-polaron representation, the enediyne structure of the TEE core is preserved, and only the nitrophenyl rings adopt a quinoid-like form.

The electron affinities computed at the Hartree-Fock level of theory are presented in Table 6. For the first reduction step an electron affinity of -1.267 eV was found (HF/PVDZa/HF/6-31G**) and for the second 1.607 eV. At B3LYP/6-31G**//HF/6-31G**, the first electron affinity is -2.367 eV, whereas the second electron affinity is found at 0.582 eV. These results clearly show that a more sophisticated electron correlation treatment is required for the computations of the electron affinities of **9**. Computations at a higher level of theory, however, are not yet easily feasible.

Even though there are empirical formulas that relate computed

(36) Spangler, C. W.; Liu, P.-K.; Havelka, K. O. In *Molecular Electronics and Molecular Electronic Devices*; Sienicki, K., Ed.; CRC Press: Boca Raton, FL, 1992; Vol. 3, Chapter 5. Brédas, J. L.; Street, G. B. *Acc. Chem. Res.* **1985**, *18*, 309-315.

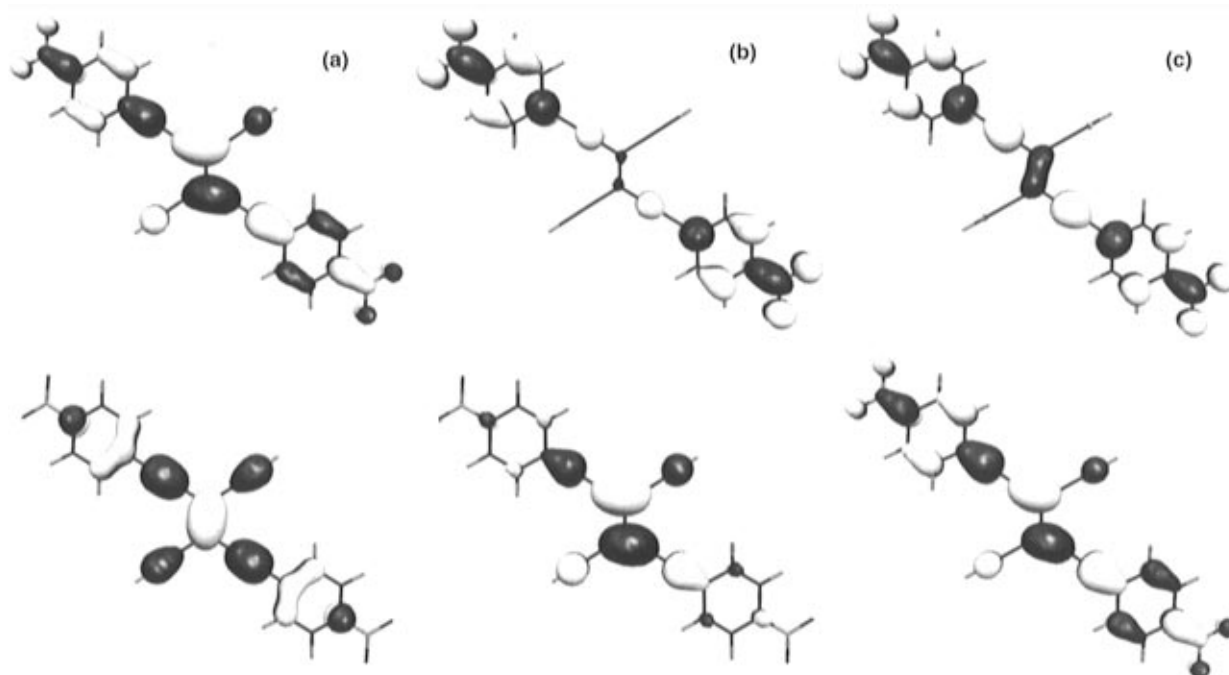
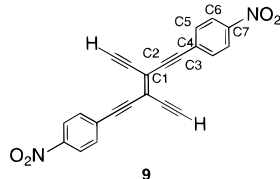


Figure 6. Highest occupied molecular orbitals (HOMOs; bottom) and lowest unoccupied molecular orbitals (LUMOs; top) of (a) neutral **9**, (b) radical anion $9^{\bullet-}$, and (c) dianion 9^{2-} .

Table 5. HF/6-31G** Mulliken Charges ($|e|$) on Selected Atoms of **9**, Radical Anion $9^{\bullet-}$, and Dianion 9^{2-} at Equilibrium Structure



atom	ne ^a	ma ^b	da ^c
C1	0.058	-0.075	-0.151
C2	0.016	0.058	0.079
C3	-0.233	-0.291	-0.242
C4	0.036	0.054	-0.003
C5	-0.122	-0.153	-0.177
C6	-0.106	-0.098	-0.084
C7	0.137	0.101	0.051
-NO ₂	-0.416	-0.491	-0.685

^a ne designates the neutral species. ^b ma designates the monoanion. ^c da designates the dianion.

electron affinities with redox potentials,³⁷ a direct comparison of these data is difficult, particularly for the second reduction step. Whereas experiments find little or no difference in the redox potentials for these two reduction steps, the computations would predict two distinct reduction potentials. We should point out, however, that the theoretical data are single-molecule (gas phase) values at 0 K with no counterions (electrolyte) involved. The introduction of the counter charges would change the situation dramatically, but again the corresponding computational effort is beyond the scope of this work.

(d) Mechanistic Considerations. A reduced bond length alternation of the enyne tether, as discussed in the previous section, is also predicted on the basis of a wealth of information derived from doping studies of polymers such as polydiacetylene or poly(phenylene)vinylene and from theoretical investigations.³⁶ The ability of acetylenes, which are known to be rather poor mediums of conjugation when compared to olefins, to participate

in such a large structural rearrangement upon reduction is, however, relatively untested. To determine the bond character and the extent of conjugation and charge delocalization, the barrier to rotation of the nitrophenyl rings about the bond connecting the TEE with the nitrophenyl group (bond *e* in the figure of Table 4) and the barrier to rotation about the central bond *h* have been computed for **9**. The calculations were performed at the HF/6-31G** level of theory starting from the planar equilibrium structure, with relaxation of the rotated species only at a torsion angle of 90°. Tables 7 and 8 show the calculated total and relative energies.

From these calculations, two conclusions can be drawn. First, it appears that the twisted (D_{2d}) form represents a saddle point between *cis*- and *trans*-isomers. Attempts to locate a twisted form lower in energy than the planar structures, by relaxation of all geometrical constraints, failed. Therefore, in contrast to similar systems such as tetraphenylethylene²² and tetracyanoethylene,³⁸ which show twisted equilibrium structures in their reduced states, compounds **8** and **9** retain planarity in all reduced states. Second, the decrease of the torsion potential about bond *h* (figure in Table 4) from 85.9 kcal/mol (a value typical for a Hartree–Fock rotational barrier about a double bond³⁹) to 5.9 kcal/mol upon reduction illustrates that the central double bond in the TEE frame acquires significant single bond character in the dianion (Table 7). Consistent with the observation of a transition toward a cumulenic structure is the increase of the torsional potential from 0.829 kcal/mol (neutral) to 28.9 kcal/mol (dianion) for the rotation about bond *e* in 9^{2-} (Table 8).

To reconcile the differing viewpoints between theory and electrochemistry, a mechanism, involving the *cis*–*trans*-isomerization of the reduced compound, emerged as outlined in Scheme 1 for the *cis*- and *trans*-enediynes model compounds **7a** and **7b**.

(38) Zheludev, A.; Grand, A.; Ressouche, E.; Schweizer, J.; Morin, B.; Epstein, A. J.; Dixon, D. A.; Miller, J. S. *J. Am. Chem. Soc.* **1994**, *116*, 7243–7249. Dixon, D. A.; Miller, J. S. *J. Am. Chem. Soc.* **1987**, *109*, 3656–3664.

(39) Hehre, W. J.; Radom, L.; Schleyer, P. v. R.; Pople, J. A. *Ab Initio Molecular Orbital Theory*; John Wiley & Sons: New York, 1986. Head-Gordon, M.; Pople, J. A. *J. Phys. Chem.* **1993**, *97*, 1147–1151.

(37) Bard, A. J.; Faulkner, L. R. *Electrochemical Methods, Fundamentals and Applications*; John Wiley & Sons: New York, 1980; Chapter 14.

Table 6. Total Energy (hartrees) and Adiabatic Energy Differences (eV) of **9**, Its Radical Anion $9^{\bullet-}$, and Dianion 9^{2-}

level of theory	$E_{\text{tot}}(\text{ne})^a$	$E_{\text{tot}}(\text{ma})^b$	$E_{\text{tot}}(\text{da})^c$
HF/6-31G**	-1246.803 313	-1246.833 336	-1246.762 003
HF/PVDZ//HF/6-31G**	-1246.878 374	-1246.914 644	-1246.847 016
HF/PVDZa//HF/6-31G**	-1246.901 901	-1246.948 476	-1246.889 405
B3LYP/6-31G**//HF/6-31G**	-1254.301 835	-1254.388 869	-1254.367 474
level of theory	$\Delta E_{\text{tot}}(\text{ma}-\text{ne})$	$\Delta E_{\text{tot}}(\text{da}-\text{ma})$	$\Delta E_{\text{tot}}(\text{da}-\text{ne})$
HF/6-31G**	-0.817	1.940	1.124
HF/PVDZ//HF/6-31G**	-0.966	1.839	0.853
HF/PVDZa//HF/6-31G**	-1.267	1.607	0.340
B3LYP/6-31G**//HF/6-31G**	-2.367	0.582	-1.785

^a ne designates the neutral species. ^b ma designates the monoanion. ^c da designates the dianion.

Table 7. Barriers to Rotation E_{rot} (kcal/mol) about the Central Bond *h* (Table 3) of **9**, Radical Anion $9^{\bullet-}$, and Dianion 9^{2-}

angle ^a (deg)	$E_{\text{rot}}(\text{ne})^b$	$E_{\text{rot}}(\text{ma})^c$	$E_{\text{rot}}(\text{da})^d$
0	0.000	0.000	0.000
30	10.501	4.286	1.673
60	40.717	16.258	4.687
90	85.922	25.194	5.925 ^e

^a All geometry parameters were kept at the values optimized for the planar equilibrium structures. ^b ne designates the neutral species. ^c ma designates the monoanion. ^d da designates the dianion. ^e The relaxation of the geometry in the dianion at 90° reduces the barrier to rotation by 0.5 kcal/mol.

Table 8. HF/6-31G** Barriers to Rotation E_{rot} (kcal/mol) about Bond *e* (Table 3) between the Nitrophenyl Rings and the TEE Core of **9**, Radical Anion $9^{\bullet-}$, and Dianion 9^{2-}

angle (deg)	$E_{\text{rot}}(\text{ne})^a$	$E_{\text{rot}}(\text{ma})^b$	$E_{\text{rot}}(\text{da})^c$
0	0.000	0.000	0.000
30	0.188	1.454	4.664
60	0.610	4.321	17.161
90	0.829	5.792	28.857

^a ne designates the neutral species. ^b ma designates the monoanion. ^c da designates the dianion.

According to the views developed above, the *cis*-enediynes **7b** is predicted to undergo a lowering of the bond length alternation in the TEE core following a one-electron transfer to each of the two nitrophenyl moieties, and the species tends toward dianion **10** with a cumulenic/quinoid structure. This pathway allows the nitrophenyl moieties to function as independent centers since the conjugation between the cumulenic “halves” in **10** and **11** is effectively impeded by the central single bond. Again, a key consideration in this mechanism is the loss of the central double bond of the enediyne framework of **7a** and **7b**, and the potential for subsequent rotation about the ensuing single bond. Rotation would then allow for isomerization of **10** to **11**, and following reoxidation, formation of **7a**.

Experimental support for the outlined redox pathway and the formation of a cumulenic type intermediate was provided through independent analysis of the electrochemical behavior of isomerically pure enediynes **7a** and **7b**. Both species **7a** and **7b** gave two reductions. The first was a two-electron reversible charge transfer as expected for reduction of the nitrophenyl groups, and the second was an irreversible one-electron charge transfer. Since **7a** and **7b** have different UV/vis absorption spectra (Figure 7c), the spectral evolution of **7b** was monitored during CV through OTTLE measurements to detect *cis*–*trans*-isomerization. Initially, the spectrum of **7b** showed characteristic absorption bands at 314 and 368 nm (Figure 7a). As the species was electrochemically reduced, these absorptions were lost, and a broad intensive band between 700 and 800 nm appeared. Reoxidation of the sample to a neutral species resulted in a spectrum with only one

absorption band at 372 nm, characteristic of the *trans*-species **7a** (Figure 7b). The possibility of photochemical isomerization⁴⁰ was disregarded, as running the spectroscopy without electrolysis resulted in no change in the spectrum of **7b**. Analogous OTTLE studies of **7a** showed that, during the course of reduction and oxidation, this species remained isomerically pure. The outcome of this experiment shows that alkynes are clearly effective in facilitating charge delocalization into the conjugated framework.

Conclusions

At first glance, the results of the electrochemical analyses of donor- and/or acceptor-functionalized tetraethynylethenes suggest that the conjugated carbon core is inefficient at delocalizing charges *between* redox centers. Thus, the first redox potentials of these molecules are essentially independent of the substitution pattern about the TEE core and/or the presence of other functionalities.

In particular, the first reduction potentials of mono- and bis-(nitrophenyl)-substituted TEEs occur at similar values, and the reduction waves have amplitudes proportional to the number of nitrophenyl groups present in the molecule. These results predict that the incurred charges are highly localized, and the nitrophenyl groups behave essentially as independent redox centers. Charge transfers at subsequent reduction potentials occur to the TEE core and *are* affected by other substituents and their orientation.

Ab initio calculations for bis(nitrophenyl)-substituted TEE **9** confirmed the independence of redox events, but also revealed a much more complex mechanism. The calculated electronic structure of the singly reduced species $9^{\bullet-}$ showed that the charge is localized on the TEE core. Only in the dianion 9^{2-} do the nitrophenyl groups accumulate considerable charge. Furthermore, we observe that the disubstituted compound retains planarity in all reduced states. This contrasts the behavior of similar compounds like tetraphenylethylene and tetracyanoethylene where three-dimensional structures are observed upon reduction. As a result of its electronic structure, the reduced species also shows considerable alternation in the bond lengths within both the phenyl rings and the TEE core. The molecule adopts a cumulenic/quinoid structure, and most importantly, the central olefinic bond acquires significant single bond character. This dramatic change in bond character in the dianion reflects the π conjugation and charge delocalization patterns that are possible in this system.

Accordingly, the barriers to rotation within the molecule also experience major changes: torsion of the nitrophenyl group about the bond to the TEE core becomes more difficult, where-

(40) (a) Anthony, J.; Knobler, C. D.; Diederich, F. *Angew. Chem.* **1993**, *105*, 437–440; *Angew. Chem., Int. Ed. Engl.* **1993**, *32*, 406–409. (b) König, B.; Schofield, E.; Bubenitschek, P.; Jones, P. G. *J. Org. Chem.* **1994**, *59*, 7142–7243.

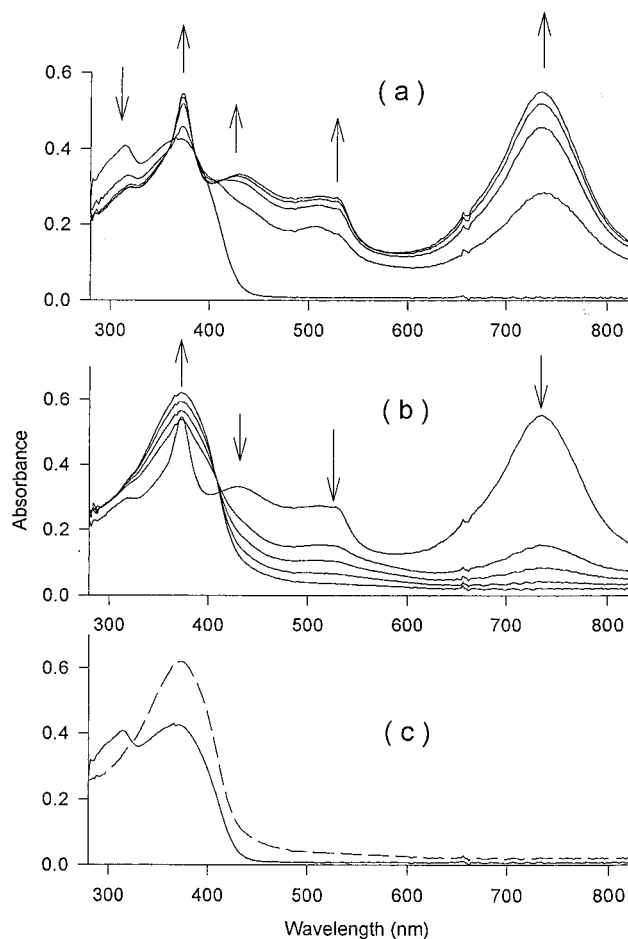
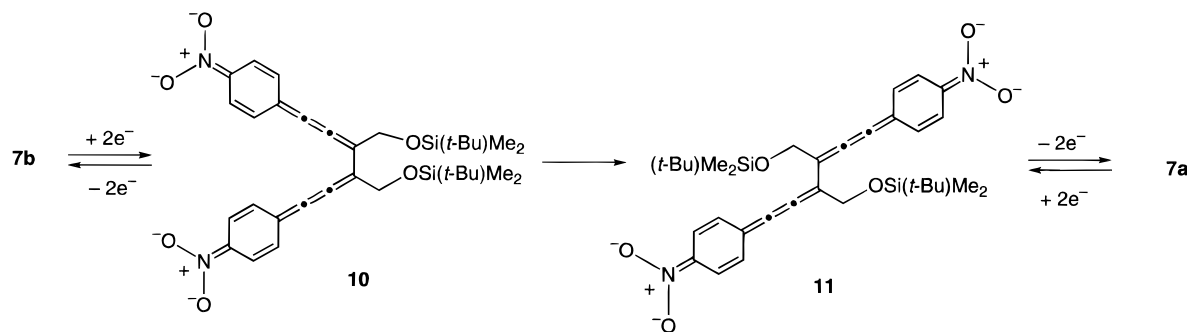
Scheme 1. Proposed Mechanism for Electrochemical *cis*–*trans*-Isomerization between Enediynes **7a** and **7b**

Figure 7. Time-resolved UV/vis spectra for the OTTLE in CH_2Cl_2 + 0.1 M Bu_4NPF_6 for (a) reduction of **7b** to dianion **10** and (b) oxidation of **11** to **7a**. (c) UV/vis spectra of **7a** (---) and **7b** (—).

as torsion about the central olefinic bond assumes a value expected for a single bond. The theoretical prediction of a cumulenyl/quinoid structure for the reduced species has been validated experimentally by the irreversible electrochemical isomerization of a *cis*-1,6-bis(4-nitrophenyl)hex-3-ene-1,5-diyne derivative to its *trans*-isomer during cyclic voltammetric reduction.

The combination of theoretical and electrochemical results provides a detailed, conclusive picture of the structural and electronic configuration of tetraethynylethenes. In particular, this study firmly establishes the ability of alkyne moieties to effectively participate in charge delocalization through a highly unsaturated carbon framework.

Experimental Section

Materials. Tetraethynylethene derivatives were synthesized as reported.^{10,11} CH_2Cl_2 was purchased spectroscopic grade from Merck, dried over molecular sieves (4 Å), and stored under argon prior to use. Tetrabutylammonium hexafluorophosphate (Bu_4NPF_6) was purchased electrochemical grade from Fluka and used as received.

Equipment. The Pt or glassy carbon disk (diameter 2 mm, EDI type, SOLEA-Tacussel, Villeurbanne, France) was used either motionless for cyclic voltammetry (CV) or as a rotating disk electrode (RDE). The electrochemical cell was connected to a computerized multipurpose electrochemical device (DACFAMOV, Microtec-CNRS, Toulouse, France) interfaced with an Apple II microcomputer. The OTTLE cell was connected to a BRUKER potentiostat (model E130M) for control and measurement of the electrochemical parameters. The UV/vis spectra were recorded with a Hewlett-Packard diode array spectrometer (model 8452A).

General Procedures. The electrochemical experiments were carried out at 20 ± 2 °C in CH_2Cl_2 containing 0.1 M Bu_4NPF_6 in a classical three-electrode cell. The working electrode was either a glassy carbon or a Pt disk electrode used either motionless for CV (10 mV s^{-1} to 10 V s^{-1}) or as a RDE. All potentials in the present study are referenced to the ferrocene/ferrocinium (Fc/Fc^+) couple which was used as an internal standard. The auxiliary electrode was a platinum wire, and a silver wire was used as a pseudoreference electrode. The accessible range of potentials was +1.2 to $-2.0 \text{ V vs Fc}/\text{Fc}^+$ on the Pt electrodes and +1.2 to $-2.2 \text{ V vs Fc}/\text{Fc}^+$ on GC in CH_2Cl_2 . Spectroelectrochemical measurements were performed in a thin layer cell (0.1 mm) through an optically transparent thin layer electrode (OTTLE) made of a Pt minigrad (1000 mesh). The auxiliary electrode was a Pt wire, and an aqueous Ag/AgCl electrode was used as the reference. The OTTLE cell was placed in a diode array UV/vis spectrophotometer.

Acknowledgment. This work was supported by the Swiss National Science Foundation (Project No. 20-40838.94), a grant from the ETH Zürich Research Council, and a postdoctoral fellowship from the U.S. Office of Naval Research (to R.R.T.). We acknowledge the generous allocations of computer resources by the ETH Zürich computer facilities.

Supporting Information Available: OTTLE spectrum for reduction of **6e**, electrochemical data and description for *p*-(*N,N*-dimethylamino)phenyl- and *p*-anisyl-substituted TEEs, and validation studies of the methods and basis sets used, with tables of the optimized geometries and energetics of parent TEE **1a** and nitrobenzene (NBZ) (6 pages). See any current masthead page for ordering and Internet access instructions.